

---

# Transformer needs NMDA receptor nonlinearity for long-term memory

---

Anonymous Author(s)

Affiliation

Address

email

## Abstract

1 The NMDA receptor (NMDAR) in the hippocampus is essential for learning and  
2 memory. We find an interesting resemblance between deep models' nonlinear  
3 activation function and the NMDAR's nonlinear dynamics. In light of a recent  
4 study that compared the transformer architecture to the formation of hippocampal  
5 memory, this paper presents new findings that NMDAR-like nonlinearity may be  
6 essential for consolidating short-term working memory into long-term reference  
7 memory. We design a navigation task assessing these two memory functions and  
8 show that manipulating the activation function (i.e., mimicking the  $Mg^{2+}$ -gating of  
9 NMDAR) disrupts long-term memory formation. Our experimental data suggest  
10 that the concept of place cells and reference memory may reside in the feed-forward  
11 network and that nonlinearity plays a key role in these processes. Our findings  
12 propose that the transformer architecture and hippocampal spatial representation  
13 resemble by sharing the overlapping concept of NMDAR nonlinearity.

## 14 1 Introduction

15 In the hippocampus, NMDAR is regarded as  
16 an essential component that mediates synaptic  
17 plasticity, memory formation, and spatial  
18 representation of place cells [9, 18, 6]. It has  
19 unique nonlinear dynamics which is modulated  
20 by  $Mg^{2+}$ -gating [13, 10], serving as a switch  
21 for synaptic plasticity and long-term memory  
22 formation [1, 17, 12] (Fig. 1a). This work is  
23 inspired by 1) the fascinating resemblance of  
24 NMDAR with the nonlinear GELU activation  
25 function that is widely used in the feed-forward  
26 networks of modern transformer architectures  
27 (Fig. 1c) [5, 4, 2] and 2) recent models relating  
28 transformer's self-attention mechanism to hip-  
29 pocampal formation [21, 20]. These findings  
30 motivated us to ask a question; **is the NMDAR-**  
31 **like nonlinearity in the feed-forward network**  
32 **of transformers required for long-term mem-**  
33 **ory formation and spatial place cell represen-**  
34 **tation?**

35 To address this question, we design a spatial  
36 navigation task in a 2D grid environment that

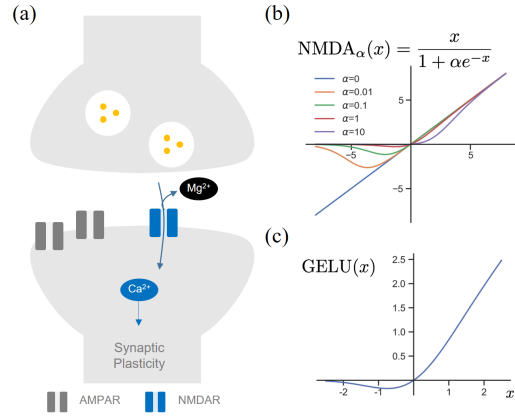


Figure 1: (a) Schematic diagram of  $Mg^{2+}$ -gated NMDAR modulating synaptic plasticity. (b)  $Mg^{2+}$ -gated NMDAR-like activation function. (c) Gaussian Error Linear Unit (GELU) activation function in transformer's feed-forward layers.

37 assesses two different memory types in neuroscience [15, 16]: working memory and reference  
 38 memory. Working memory controls the events from a within-trial, while reference memory controls  
 39 across-trials from the unchanging environment. Our experimental data suggest that NMDAR-like  
 40 nonlinearity in feed-forward networks of the transformer is essential for reference memory formation  
 41 and place cell representation.

## 42 2 Methods

43 **Relating activation function in transformers with NMDAR nonlinearities** NMDAR’s nonlinear  
 44 dynamics arises from the voltage-gated  $Mg^{2+}$  repulsion at the NMDAR channel’s pore [13, 10]  
 45 (Fig. 1a). Previously,  $Mg^{2+}$ -gated NMDAR open probability  $p$  has been shown to follow ion blockade  
 46 model of A where  $x$  represent an input voltage,  $\alpha = [Mg^{2+}]/K_{Mg^{2+}}$  is a parameter determined by  
 47  $[Mg^{2+}]$ ,  $K_{Mg^{2+}}$  is a dissociation constant, and  $\beta$  is a temperature constant. As experimentally shown,  
 48 increasing the  $Mg^{2+}$  level in the brain can enhance long-term memory formation [17]. We observed  
 49 the NMDAR’s nonlinear dynamics of the *IV* curve (current-voltage relationship) in the synapse  
 50 to closely resemble the form of the GELU activation function. GELU is a widely used activation  
 51 function in transformers (Fig. 1c;  $GELU(x) \approx x\sigma(1.702x)$  where  $\sigma$  is the sigmoid function) [5, 4, 2].  
 52 Inspired by this resemblance, we define a new nonlinear activation function (Fig. 1b) with  $\alpha$  parameter  
 53 which modulates dynamics as follows:

$$NMDA_\alpha(x) = x p_\alpha(x) = \frac{x}{1 + \alpha e^{-x}}. \quad (1)$$

54 To investigate this NMDAR-like nonlinearity in transformer memory formation, we replaced the  
 55 GELU( $x$ ) activation function with  $NMDA_\alpha(x)$  in a standard transformer model.

### 56 Transformers learn spatial navigation tasks

57 We train the transformer model to predict the subsequent sensory observation of an agent that  
 58 randomly walks a 2D grid environment [20]  
 59 (Fig. 2). A sequence of previous [Action ( $a$ ),  
 60 Observation ( $x$ )] pairs are an input to the model,  
 61 and the subsequent observation is masked for  
 62 prediction. Instead of using positional encoding  
 63 [19] that is commonly used in transformers,  
 64 we employ the recurrent neural network (RNN)  
 65 for encoding the sequence of actions [20]<sup>1</sup>.  
 66

67 We generate the embedding vectors of sensory  
 68 observation ( $x$ ) sequence with a word embed-  
 69 ding layer, but the embedding vectors of the  
 70 action sequence is generated by RNN;  $e_{t+1} =$   
 71  $\tanh(e_t W_a)$ , where  $e_t$  is the positional embed-  
 72 ding at step  $t$ , and  $W_a$  is the action-dependent  
 73 trainable weight matrix. The input is given by  
 74  $\{[x_1, e_1], [x_2, e_2], \dots, [x_t, e_t]\}$ ; the initial pos-  
 75 i-tional embedding  $e_1$  is sampled from a normal distribution and we mask the last observation  $x_t$ . We  
 76 generate  $N$  maps of  $11 \times 11$  2D grids. A random sensory observation among ten letters is placed at  
 77 each position on each map. Agents can move ‘up’, ‘right’, ‘down’, ‘left’, or ‘stay’. An agent starts at  
 78 a random position and initiates a random walk on the map for 2,048 steps for each trial.

79 The model is trained with the softmax cross-entropy loss and predicts the subsequent sensory  
 80 observation (i.e., dotted squares). We evaluate two types of memory: **working memory (WM)**  
 81 and **reference memory (RM)**<sup>2</sup>. When the prediction on nodes that were previously visited during  
 82 the random walking is incorrect, it will count as a WM error (see Fig. 2 left). On the other hand,  
 83 when the prediction on unvisited nodes is incorrect, it will count as a RM error (see Fig. 2 right).  
 84 Minimizing the RM error by memorizing input sequences is infeasible; the possible number of

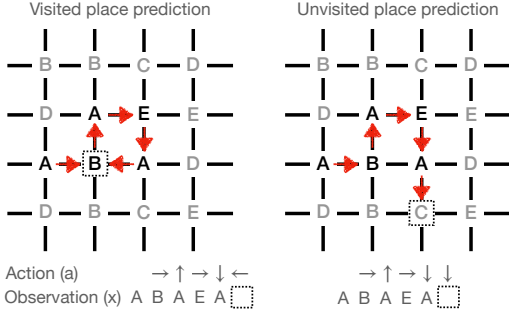


Figure 2: Sensory observation prediction task in a 2D grid, where dotted squares indicate the target position to predict given a sequence of past actions and observations. Gray (black) letters represent the unvisited (visited) places.

<sup>1</sup>Encoding actions with RNN is closely related to the state-of-the-art neuroscience model of hippocampus.

<sup>2</sup>Whittington et al. [20] only evaluated the WM error based on our definitions of WM and RM.

85 sequence configurations is exponential since the input sequence is randomly generated at each trial.  
 86 To solve this task, the model should be able to 1) understand the abstract structure of 2D space, 2)  
 87 infer which map it is on from input sequence data, and 3) memorize what sensory observation is  
 88 placed at each position in that map. See Appendix A.1 for training, evaluation, and transformer model  
 89 details.

### 90 3 Results

91 **WM error & RM error** The feed-forward network (FFN; see Fig. 4a) in the transformer model  
 92 consists of two linear layers with the NMDAR-inspired activation function  $\text{NMDA}_\alpha$  (Eq. (1)). To  
 93 measure the impact of non-linearity  $\alpha$  in FFNs, we train the transformer models with different  
 94 values of  $\alpha$  in  $[0, 0.01, 0.05, 0.1, 0.5, 1, 5, 10]$  and evaluate WM and RM errors on the train maps (i.e.,  
 95 familiar maps) and test maps (i.e., novel maps).

96 Figure 3a shows that the RM error on the train maps is rapidly decreased over train trials when  $\alpha$   
 97 is larger than zero, with a larger improvement for increasing  $\alpha$ . The RM error on the novel maps,  
 98 however, is nearly constant at 0.9 ( $= 1 - 1/(\text{number of letters})$ ) for all  $\alpha$ . Unlike the RM, Fig. 3a  
 99 inset shows that WM is performing well on novel maps, which had not been shown during the  
 100 training. This finding suggests that RM is not used for predicting the visited nodes. Training the  
 101 models on different numbers of maps  $N$ , Fig. 3b shows that increasing  $\alpha$  helps improve RM and the  
 102 trend of improvement is consistently shown for  $N = 32, 48$ , and  $64$  cases. As  $N$  grows, the RM  
 103 error increases as more ‘what’-‘where’ (letter-place) pairs have to be memorized.

104 **Place cells in FFNs** Place cell is a neuron in the hippocampus which fires at a particular place of  
 105 the environment [14]. Selective impairment of NMDAR in hippocampal CA1 disrupts place cell  
 106 emergence and long-term memory formation [18, 6, 11]. We investigate the role of neurons in FFNs  
 107 and self-attention layers by measuring the neuron’s place specificity. We measure the place cell score  
 108 by defining a  $K \times K$  2D grid environment as graph  $G = (V, E)$  and building a sub-graph  $\mathcal{G} = (\mathcal{V}, \mathcal{E})$   
 109 of all connected components from the source node  $i_{\max}$  where the neuron fires maximally; directed  
 110 edges of sub-graph  $\mathcal{G}$  are generated by connecting high to low firing nodes. We run depth-first-search  
 111 from  $i_{\max}$ . Given  $G$  and  $\mathcal{G}$ , the place cell score is

$$\text{Place cell score} = \gamma \frac{\sum_{i \in \mathcal{V}} \rho_i}{\sum_{i \in V} \rho_i}, \quad (2)$$

112 where  $\gamma = 1 - |\mathcal{V}^*|/|V|$  is a discount factor and  $\mathcal{V}^*$  is a set of nodes from sub-graph without  $i_{\max}$   
 113 and leaf nodes during depth-first search.  $\rho_i$  denotes a firing rate at node  $i$ . We record the firing  
 114 rate  $\rho_i$  of neurons over a random walking trajectory with  $10^5$  steps in one of the training maps.  
 115 Then we measure the place cell scores of neurons in FFNs and self-attention layers. The place cell  
 116 score is 1 when the neuron is firing only at a certain node; the score is 0 when the neuron is firing  
 117 homogeneously across all nodes.

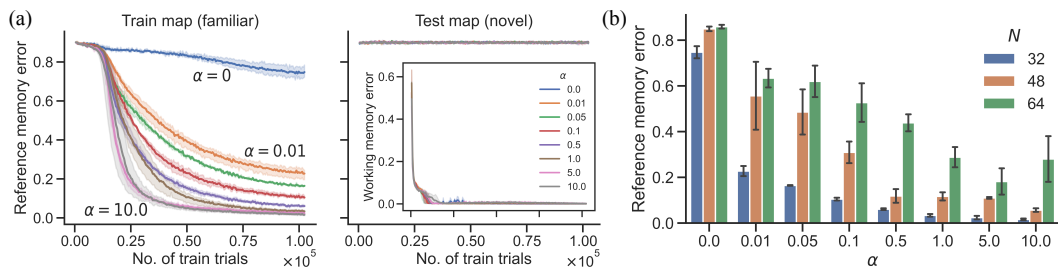


Figure 3: (a) Reference memory errors over training trials for training (familiar) maps and testing (novel) maps for  $N = 32$  where  $N$  is the number of training maps. Inset: working memory errors on the novel maps over training trials. (b) Reference memory errors over different values of  $\alpha$  and  $N$ . Error bars and shaded areas represent the standard deviation of errors from three independently trained models.

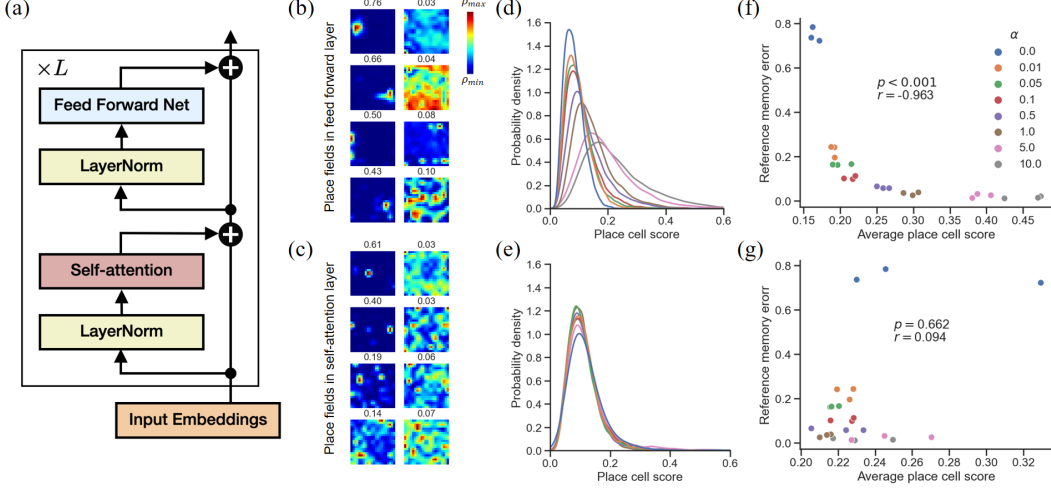


Figure 4: Reference memory-related place cells selectively emerge in the feed-forward layer but not in the self-attention layer along with  $\alpha$  increase. (a) The transformer architecture used in the current study. (b, c) Example rate maps with place scores in feed-forward layers and self-attention layers at  $\alpha = 10$ ; from top left (high) to bottom right (low) (d) Place cell score distribution in feed-forward layers change along with  $\alpha$  modulation. (e) Place cell score distribution in self-attention layers does not change along with  $\alpha$  modulation. (f-g) Scatter plot of average place cell scores and reference memory errors.  $r$  and  $p$  denote Spearman’s rank correlation coefficient and significance score, respectively.

Fig. 4b and 4c show the rate maps of neurons with place cell scores in the FFNs and self-attention layers, respectively (Fig. 4a). As can be seen, our metric well represents place specificity. Fig. 4d and 4e show the distribution of place cell scores in FFNs and self-attention layers with different values of  $\alpha$ . As we increase  $\alpha$ , the place cell score distribution found in FFNs gets positively shifted (see Fig. 5 for rate maps for  $\alpha = 0, 1.0$ , and  $10.0$  in Appendix A.2), whereas place cell score distribution in the self-attention layers remains. In addition, Fig. 4f and 4g show a relationship between the average place cell score and RM error for each  $\alpha$ . While average place cell scores in the self-attention layer show no correlation with RM errors whatsoever, neurons in the FFN layer exhibit substantial correlation. These results imply that NMDAR-like nonlinearity in FFNs induces RM formation and the emergence of place cells.

## 4 Discussion and Conclusion

Whittington et al. [20] showed that softmax neurons in the self-attention layer behave like place cells and demonstrated that changing the softmax function to linear slows the WM learning process. However, the role of neurons in FFNs has not been studied. We demonstrate for the first time that place cells could emerge in transformers’ FFNs, which we show by testing the emergence of place cells in FFNs with an NMDA-inspired activation function. Even though there are trainable parameters in the self-attention layer, the quantitative analysis of the place cell score indicates that most of the RM is stored in FFNs. Our results agree qualitatively with previous NMDAR impairment experiments from neuroscience: 1) hippocampal CA1 NMDAR perturbation does not impair WM [8], 2) changing NMDAR  $Mg^{2+}$ -gating (changing  $\alpha$  in this work) enhances or disrupts long-term memory formation [17, 12], 3) NMDAR is required for long-term stabilization of newly forming place fields [11, 6]. Our contribution is at showing these patterns experimentally for the first time.

Our research has exciting future directions. The current study only examined what-where memory using a sensory observation task in a static environment. However, our real-world environment is changing dynamically. Unfortunately, modern deep learning systems are generally incapable of adapting to a dynamic environment or reordering sensory inputs. In future work, we intend to explore what-where-when memory, called *episodic memory*, in transformer and other deep models.

145 **References**

- 146 [1] Tim VP Bliss and Graham L Collingridge. A synaptic model of memory: long-term potentiation  
147 in the hippocampus. *Nature*, 361(6407):31–39, 1993.
- 148 [2] Tom Brown, Benjamin Mann, Nick Ryder, Melanie Subbiah, Jared D Kaplan, Prafulla  
149 Dhariwal, Arvind Neelakantan, Pranav Shyam, Girish Sastry, Amanda Askell, Sandhini  
150 Agarwal, Ariel Herbert-Voss, Gretchen Krueger, Tom Henighan, Rewon Child, Aditya  
151 Ramesh, Daniel Ziegler, Jeffrey Wu, Clemens Winter, Chris Hesse, Mark Chen, Eric  
152 Sigler, Mateusz Litwin, Scott Gray, Benjamin Chess, Jack Clark, Christopher Berner, Sam  
153 McCandlish, Alec Radford, Ilya Sutskever, and Dario Amodei. Language models are  
154 few-shot learners. In *Advances in Neural Information Processing Systems*, volume 33,  
155 pages 1877–1901, 2020. URL <https://proceedings.neurips.cc/paper/2020/file/1457c0d6bfcb4967418bfb8ac142f64a-Paper.pdf>.
- 157 [3] Zihang Dai, Zhilin Yang, Yiming Yang, Jaime G. Carbonell, Quoc Viet Le, and Ruslan Salakhut-  
158 dinov. Transformer-xl: Attentive language models beyond a fixed-length context. In *Association  
159 for Computational Linguistics*, pages 2978–2988, 2019.
- 160 [4] Jacob Devlin, Ming-Wei Chang, Kenton Lee, and Kristina Toutanova. Bert: Pre-training of  
161 deep bidirectional transformers for language understanding. *arXiv preprint arXiv:1810.04805*,  
162 2018.
- 163 [5] Dan Hendrycks and Kevin Gimpel. Gaussian error linear units (gelus). *arXiv preprint  
164 arXiv:1606.08415*, 2016.
- 165 [6] Clifford Kentros, Eric Hargreaves, Robert D Hawkins, Eric R Kandel, Matthew Shapiro, and  
166 Robert V Muller. Abolition of long-term stability of new hippocampal place cell maps by nmda  
167 receptor blockade. *Science*, 280(5372):2121–2126, 1998.
- 168 [7] Diederik P. Kingma and Jimmy Ba. Adam: A method for stochastic optimization. In *International  
169 Conference on Learning Representations*, 2015. URL <http://arxiv.org/abs/1412.6980>.
- 171 [8] Inah Lee and Raymond P Kesner. Differential contribution of nmda receptors in hippocampal  
172 subregions to spatial working memory. *Nature neuroscience*, 5(2):162–168, 2002.
- 173 [9] Fei Li and Joe Z Tsien. Memory and the nmda receptors. *The New England journal of medicine*,  
174 361(3):302, 2009.
- 175 [10] Mark L Mayer, Gary L Westbrook, and Peter B Guthrie. Voltage-dependent block by mg2+ of  
176 nmda responses in spinal cord neurones. *Nature*, 309(5965):261–263, 1984.
- 177 [11] Thomas J McHugh, Kenneth I Blum, Joe Z Tsien, Susumu Tonegawa, and Matthew A Wilson.  
178 Impaired hippocampal representation of space in ca1-specific nmdar1 knockout mice. *Cell*, 87  
179 (7):1339–1349, 1996.
- 180 [12] Tomoyuki Miyashita, Yoshiaki Oda, Junjiro Horiuchi, Jerry CP Yin, Takako Morimoto, and  
181 Minoru Saitoe. Mg2+ block of drosophila nmda receptors is required for long-term memory  
182 formation and creb-dependent gene expression. *Neuron*, 74(5):887–898, 2012.
- 183 [13] LPPAA Nowak, P Bregestovski, P Ascher, A Herbet, and Aa Prochiantz. Magnesium gates  
184 glutamate-activated channels in mouse central neurones. *Nature*, 307(5950):462–465, 1984.
- 185 [14] John O’Keefe and Jonathan Dostrovsky. The hippocampus as a spatial map: Preliminary  
186 evidence from unit activity in the freely-moving rat. *Brain research*, 1971.
- 187 [15] David S Olton, Christine Collison, and Mary Ann Werz. Spatial memory and radial arm maze  
188 performance of rats. *Learning and motivation*, 8(3):289–314, 1977.
- 189 [16] David S Olton, James T Becker, and Gail E Handelmann. Hippocampus, space, and memory.  
190 *Behavioral and Brain sciences*, 2(3):313–322, 1979.

- 191 [17] Inna Slutsky, Nashat Abumaria, Long-Jun Wu, Chao Huang, Ling Zhang, Bo Li, Xiang Zhao,  
 192 Arvind Govindarajan, Ming-Gao Zhao, Min Zhuo, et al. Enhancement of learning and memory  
 193 by elevating brain magnesium. *Neuron*, 65(2):165–177, 2010.
- 194 [18] Joe Z Tsien, Patricio T Huerta, and Susumu Tonegawa. The essential role of hippocampal ca1  
 195 nmda receptor-dependent synaptic plasticity in spatial memory. *Cell*, 87(7):1327–1338, 1996.
- 196 [19] Ashish Vaswani, Noam Shazeer, Niki Parmar, Jakob Uszkoreit, Llion Jones, Aidan N Gomez,  
 197 Łukasz Kaiser, and Illia Polosukhin. Attention is all you need. *Advances in neural information  
 198 processing systems*, 30, 2017.
- 199 [20] James C. R. Whittington, Joseph Warren, and Tim E.J. Behrens. Relating transformers to models  
 200 and neural representations of the hippocampal formation. In *International Conference on Learn-  
 201 ing Representations*, 2022. URL <https://openreview.net/forum?id=B8DV09B1YE0>.
- 202 [21] James CR Whittington, Timothy H Muller, Shirley Mark, Guifen Chen, Caswell Barry, Neil  
 203 Burgess, and Timothy EJ Behrens. The tolman-eichenbaum machine: unifying space and  
 204 relational memory through generalization in the hippocampal formation. *Cell*, 183(5):1249–  
 205 1263, 2020.

206 **Checklist**

- 207 1. For all authors...
  - 208 (a) Do the main claims made in the abstract and introduction accurately reflect the paper's  
   209 contributions and scope? **[Yes]** See Abstract and Introduction.
  - 210 (b) Did you describe the limitations of your work? **[Yes]** See Discussion section.
  - 211 (c) Did you discuss any potential negative societal impacts of your work? **[N/A]**
  - 212 (d) Have you read the ethics review guidelines and ensured that your paper conforms to  
   213 them? **[Yes]** Yes, I read it and this paper conforms to them.
- 214 2. If you are including theoretical results...
  - 215 (a) Did you state the full set of assumptions of all theoretical results? **[N/A]**
  - 216 (b) Did you include complete proofs of all theoretical results? **[N/A]**
- 217 3. If you ran experiments...
  - 218 (a) Did you include the code, data, and instructions needed to reproduce the main experi-  
   219 mental results (either in the supplemental material or as a URL)? **[Yes]** All training,  
   220 evaluation, and model details have been specified in the text. The code will be released  
   221 with the camera-ready version.
  - 222 (b) Did you specify all the training details (e.g., data splits, hyperparameters, how they  
   223 were chosen)? **[Yes]** See Appendix A.1
  - 224 (c) Did you report error bars (e.g., with respect to the random seed after running experi-  
   225 ments multiple times)? **[Yes]** We ran 3 different random seeds.
  - 226 (d) Did you include the total amount of compute and the type of resources used (e.g., type  
   227 of GPUs, internal cluster, or cloud provider)? **[Yes]** See Appendix A.1.
- 228 4. If you are using existing assets (e.g., code, data, models) or curating/releasing new assets...
  - 229 (a) If your work uses existing assets, did you cite the creators? **[N/A]**
  - 230 (b) Did you mention the license of the assets? **[N/A]**
  - 231 (c) Did you include any new assets either in the supplemental material or as a URL? **[N/A]**
  - 232 (d) Did you discuss whether and how consent was obtained from people whose data you're  
   233 using/curating? **[N/A]**
  - 235 (e) Did you discuss whether the data you are using/curating contains personally identifiable  
   236 information or offensive content? **[N/A]**
- 237 5. If you used crowdsourcing or conducted research with human subjects...
  - 238 (a) Did you include the full text of instructions given to participants and screenshots, if  
   239 applicable? **[N/A]**

- 240                   (b) Did you describe any potential participant risks, with links to Institutional Review  
 241                   Board (IRB) approvals, if applicable? [N/A]  
 242                   (c) Did you include the estimated hourly wage paid to participants and the total amount  
 243                   spent on participant compensation? [N/A]

244           **A Appendix**

245           **A.1 Training, evaluation, and model configuration details**

246           All runs used the same training method and model configuration except for the nonlinearity  $\alpha$  of  
 247           NMDA $_\alpha$  activation function. We used TransformerXL [3] with an extended memory length of 32  
 248           and segment length of 32 so that working memory error is measured within a sequence length of  
 249           65( $= 64 + 1$ ; 1 for the masked sensory input); i.e. a node that the agent had never visited within recent  
 250           64 steps is treated as an unvisited node. The model consisted of two layers with a word embedding  
 251           dimension of 256 and a positional embedding size of 256. The input embedding is concatenated  
 252           vector  $[x, e]$  of the word embedding  $x$  and positional embedding  $e$  so that the input embedding  
 253           dimension is 512. The number of heads in the self-attention layer is 8 and the number of neurons in  
 254           the feed forward net (FFN) is 2,048. The dropout rate is set to 0.1 and the maximum clip norm of  
 255           gradient is set to 0.25. We employed ADAM [7] optimizer and a learning rate schedule with a linear  
 256           decay from 0.0001 (start) to 0 (end). We ran 512 random walk simulations in parallel for collecting  
 257           training trajectories. The total number of random walking steps is 2,048 for each simulation so the  
 258           total number of gradient steps for each run was 512 (batch size)  $\times$  2,048 (total number of steps in a  
 259           trial)  $\times$  200 (number of trials). All runs were performed on a single NVIDIA TITAN V GPU.

260           **A.2 Analysis details of place cell distribution in transformer**

261           We plot each place cell score distribution with neurons from 3 independent experiments. For the  
 262           self-attention layer, the total number of neurons in the softmax layer is 65 (number of sequence  
 263           length)  $\times$  8 (number of head)  $\times$  2 (number of layers). For the feed-forward networks, the total  
 264           number of neurons in the feed-forward layer is 2048 (number of neurons)  $\times$  2 (number of layers).  
 265           Rate maps of neurons with top-64 place scores in FFNs with varying  $\alpha$  are shown in Figure 5.

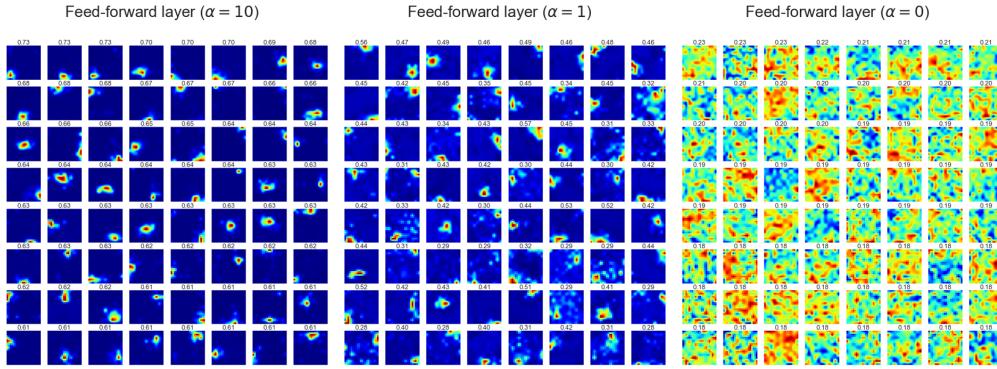


Figure 5: Rate maps of neurons with top-64 place scores in FFNs with varying values of  $\alpha$ ;  $\alpha = 10$  (left),  $\alpha = 1$  (middle), and  $\alpha = 0$  (right).